Leadership in Sustainable Infrastructure
Leadership en Infrastructures Durables

Vancouver, Canada
May 31 – June 3, 2017/ *Mai 31 – Juin 3, 2017*

NUMERICAL ANALYSIS OF STEEL SLIT DAMPERS UNDER CYCLIC LOADING

Madheswaran, Jayanthan[1,3] and Tesfamariam, Solomon[2,4]
[1, 2] The University of British Columbia, Kelowna, Canada
[3] jayanthan.madheswaran@alumni.ubc.ca
[4] solomon.tesfamariam@ubc.ca

Abstract: Dampers have been widely incorporated in the structure to enhance its seismic performance during earthquake action. Among those, steel slit damper, a type of "metallic damper" which can dissipate energy through bending or shear deformation is considered in this study. Since, width of these strips is same for entire height, damages are mainly concentrated at the end strips due to high stress. The aim of this study is to identify the suitable geometric configuration of damper which can perform better during structural application, in terms of strength, ductility and energy dissipation capacity. For this purpose, a conventional steel slit damper is numerically simulated using ABAQUS software subjected to reverse cyclic loading and validated with experimental result. Further, a detailed parametric study is carried out to reduce stress concentration on the width of strips to obtain the optimal shape for damper. In addition to that, the effect of parameter interaction and their influence in the final response is also studied using factorial design of experiments and with that predictive equation is developed using response surface method. Finally, structural characteristics of dampers for different configuration will be evaluated to consider best one for the use in real life structure for retrofitting.

INTRODUCTION

Dampers are passive control systems or passive energy dissipation devices that are implemented in the structures to protect against seismic excitation. These passive control systems are categorized based on their dissipative mechanisms: metallic (Skinner et al. 1973), friction (Pall et al. 1980), viscous fluid (Constantinou et al. 1993) and viscoelastic (solid) dampers (Chang et al. 1995). Metallic dampers dissipate the energy through inelastic deformation and provide a stable hysteretic envelope. Based on axial, shear and flexural yielding mechanism, several metallic damper designs have been proposed by researches, such as added damping and stiffness (Bergman et al. 1987), triangular added damping and stiffness (Tsai et al. 1993), honeycomb damper (Kobori et al. 1992) and steel slit damper (Chan et al. 2008). Though all dampers were incorporated within the bracing system of structural frame, but steel slit damper can be used as a connection element between the beam and column junction in steel frames because of its high stiffness and excellent energy dissipating capacity (Oh et al. 2009). This device dissipates the energy through flexural yielding of strips. The strips are made by cutting number of slits along the longer direction of the damper. This study aims in finding the effect of different parameters on slit dampers using design of experiment technique.

In recent years, several investigations have been made on finding the appropriate design of slit damper. Chan et al. (2008) developed slit damper with different strip configuration and performed low cycle fatigue test. The result provides good energy dissipation capacity but damage is brittle in nature (Figure 1).

Ghabraie et al. (2010) identified that the brittle failure is due to accumulation of stress concentration in strip ends and optimized the shape of strip. Further, Lee et al. (2015) proposed three non-uniform steel strip dampers (dumbbell shaped strip, tapered strip and hourglass shape strip) which showed increased cyclic performance with stable hysteretic behaviour and cracks were evenly distributed along the strips. Teruna et al. (2015) developed four steel plates for different configuration to minimize the stress concentration by rounding the end of slits. Although experimental results from previous study indicated very stable hysteretic behaviour, there is lack of research in finding out the optimal shape of the damper with regard to height to width ratio (Lee et al. 2015, Teruna et al. 2015).

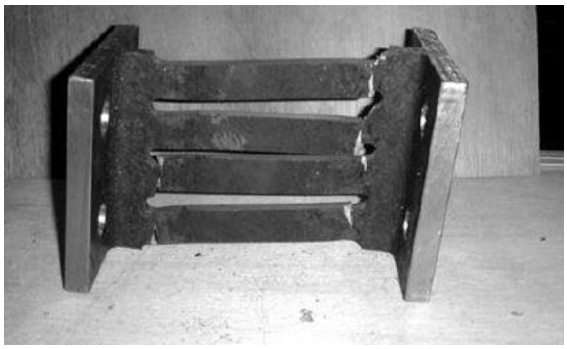

Figure 1: Damage at the strip ends due to stress concentration (adapted from Chan et al. 2008)

The Lee et al. (2015) slit dampers is used as a base line in this study. The study entails:

- A conventional steel slit damper is modeled using finite element analysis program (ABAQUS) and validated with experimental result.
- Effects of different parameters are investigated on the performance of the slit damper by constructing a factorial design of experiments. The factors considered are: Strip width at mid height (b_c), height of the strip (h) and thickness of the damper (t).
- Response surface methodology was used to formulate the relationship to understand about the parameters effects and their interactions in the response on effective stiffness and damping.

1 Numerical Investigation

In this work, a conventional strip damper with the geometrical shape (PSD-5) proposed by Lee et al. (2015) is considered (Figure 2a). They used SS 400 grade steel for the damper because of low cost and widely available in building structures. The dimensions of the specimen are: width w = 500mm, overall height H = 360mm and thickness t = 10mm. Lee et al. (2015) performed displacement based cyclic loading test to evaluate the cyclic performance of the damper. During the test, bottom region of specimen was bolted and top zone of the specimen (Figure 2b) was subjected to increasing displacements at every step with the loading rate ranges 0.1 to 0.5mm/sec. The loading sequence is shown in Figure 3. The hysteretic response obtained from the tested specimen is shown in Figure 4b.

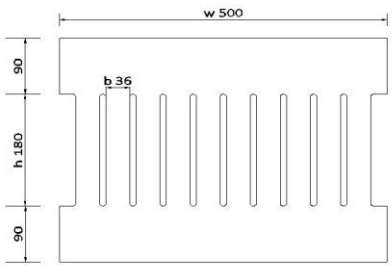

Figure 2 Steel slit damper: (a) Specimen Geometry and (b) Test set up (adapted from Lee et al. 2015)

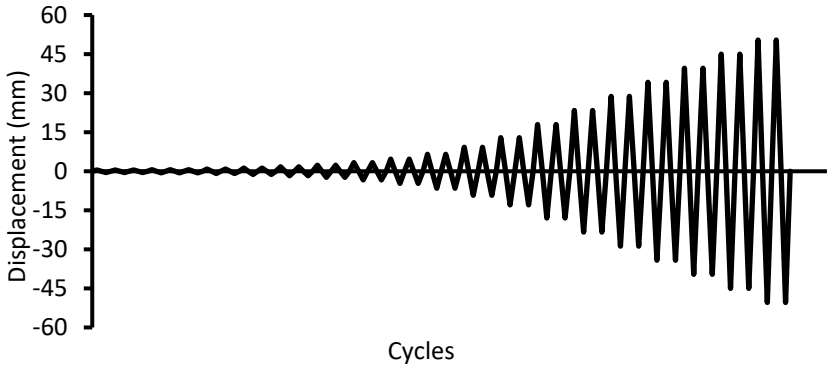

Figure 3: Cyclic loading Protocol

The numerical investigation is carried out using ABAQUS program to validate the experimental result. The damper is modeled using 8-node linear brick element (C38R) with reduced integration and hourglass control. The elastic-plastic behaviour of the steel is modelled using combined isotropic and kinematic hardening model proposed by Chaboche (1989). The hardening parameters Q, C, ɣ and b are obtained from Yoshida et al. (2004) and are summarized in Table 1. The whole element is partitioned into different cells to avoid mesh irregularities and overlapping. To avoid convergence issue, the stress concentration regions are meshed finely in order to ensure the model accuracy. Figure 4(a) shows the conventional slit damper modeled in ABAQUS program. The cyclic loading was applied at top end of the specimen by using reference point with constrain equation and bottom zone is fixed in all direction. The displacement was incremented at every steps by using static general step function and initial step size maintained at 0.01 to avoid convergence issue. Figure 4(b) depicts the hysteresis curve obtained for steel damper modeled in finite element model is in good agreement with the experimental results.

Table 1: Material Properties of steel slit damper (Yosida et al. 2004)

	Yield stress, (MPa)	Q (MPa)	C (MPa)	ɣ (Gamma)	b	Young's Modulus (MPa)	Poisson ratio
SS-400	250	75	5,880	55	13.5	207,000	0.3

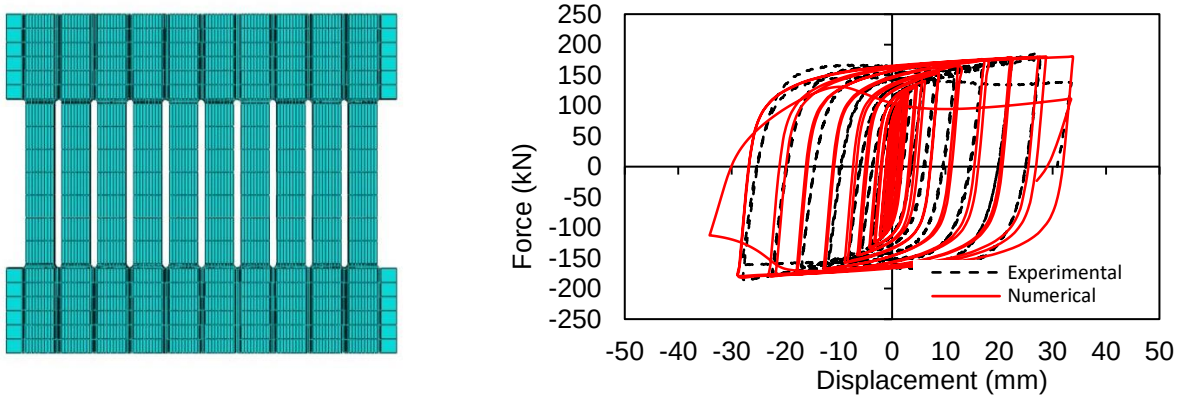

(a) (b)

Figure 4 Steel slit damper: (a) Finite Element Model and (b) Hysteretic Response

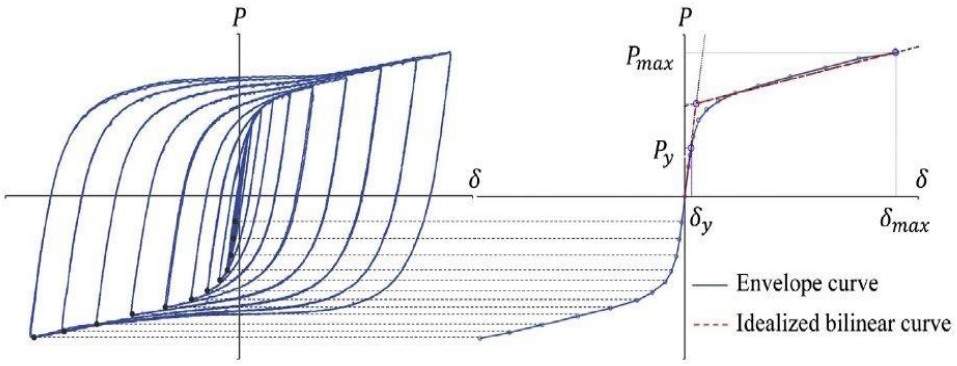

Figure 5: Hysteresis and their bilinear curve idealization (adapted from Lee et al. 2015)

After obtaining the hysteretic curves (e.g. Figure 4b), structural characteristics of the damper were evaluated with bilinear curve by connecting the maximum loading point at each step before the failure. From the bilinear curve, yield load (P_y) and yield displacement (δ_y) points were found out by intersecting line drawn from the initial behaviour and line touching the envelope curve (Figure 5). Since, metals are rate independent under cyclic loading. Nonlinear properties of the damper performance are expressed in terms of equivalent stiffness (K_{eff}) and effective damping (β_{eff}) is calculated using equation [1] and [2], respectively.

[1] $$K_{eff} = \frac{|P_{max}| + |P_{min}|}{|\delta_{max}| + |\delta_{min}|}$$

[2] $$\beta_{eff} = \frac{2}{\pi} \frac{E_{loop}}{K_{eff}\left(|\delta_{max}| + |\delta_{min}|\right)}$$

where, P_{max} and P_{min} – maximum and minimum loads, δ_{max} and δ_{min} – maximum and minimum displacements and E_{loop} – energy dissipated per cycle. The parameters required for stiffness and damping are obtained from the hysteresis envelope is illustrated in Figure 6.

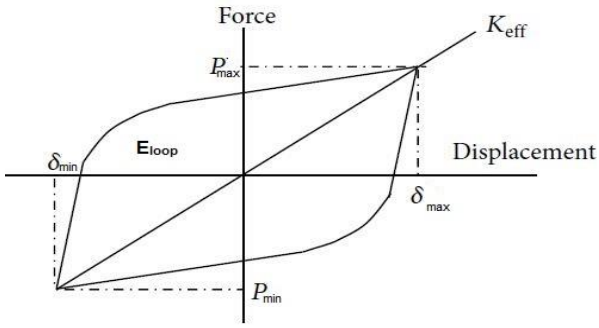

Figure 6: Stiffness and Damping characteristics

2 Parametric Study

To reduce the stress concentration in the damper, conventional geometrical shape is modified to find the optimal shape of the damper. A detailed parametric study has been carried out using a design of experiment technique. Three shape variables each with three levels were chosen by considering overall performance of the damper are given in Table 2. Based on chosen variables and levels, 3^3 full factorial design of experiment is constructed with the total number of 27 runs are given in Table 3. The Shape parameters b_c, h and t are presented in Figure 7. Further, strip width at the top (b) is made constant for all specimens and height of damper is chosen based on aspect ratio (h/b_c) which varies from 2.5 to 7.5.

Table 2: Parameter and their levels considered in sensitivity analysis

Factor	Level		
	1	2	3
Strip width at the mid height (b_c), mm	9	18	36
Height of strip (h), mm	90	180	270
Thickness (t), mm	10	15	20

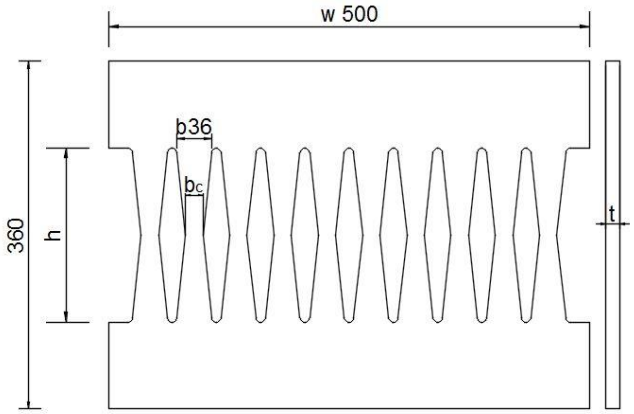

Figure 7: Shape Parameters

Based on the parameter combinations, 27 geometrical shapes were modeled with the validated material properties according to design mentioned in Table 3. Figure 8, 9 and 10 shows the FE model and their hysteretic responses for typical parameter combinations considering different strip height with same strip width at mid height and thickness. After subjecting the model to displacement loading, the structural characteristics were computed from the hysteretic responses is summarised in Table 3. From Figure 8 hysteretic response reveals that load increased abruptly at small displacement and specimen fails at early stage. The reason for this failure is due to increased stiffness of the specimen. Figure 9 and 10 shows the response from the specimen with increased strip height which provides the stable hysteretic envelope by undergoing larger deformation and enhances the energy dissipation capacity. On comparing hysteretic responses of three different strip heights, specimen with h=270mm yielded around 65 kN and exhibited a stable hysteretic behaviour until displacement of 34mm. The stress concentration in conventional damper is not evenly distributed and concentrated only at strip ends, which leads to specimen to fail at early stage. If the damper shape is modified by reducing the width at the mid height (Figure 8, 9 and 10), the stresses are distributed through the strip height and avoids the stress localization. Because of this effect, the cracks will be propagating along the strip height rather than at the one end.

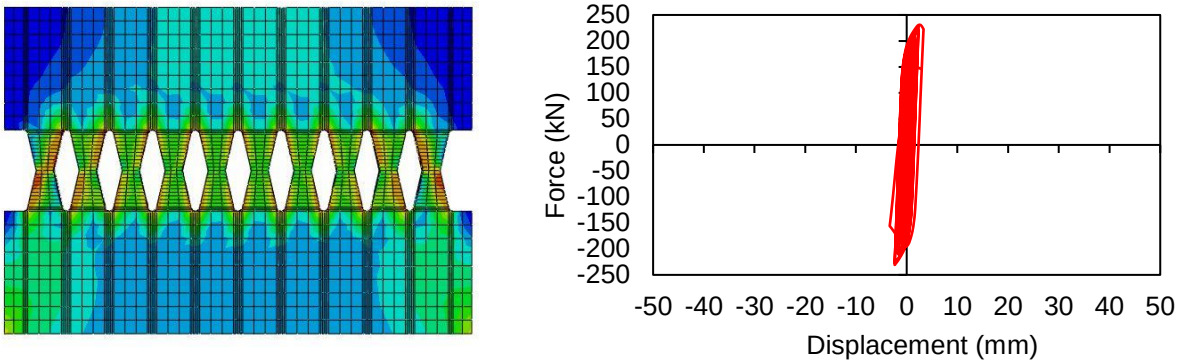

Figure 8: FE model and Hysteretic response for damper with b_c = 18mm, h = 90mm and t = 10mm

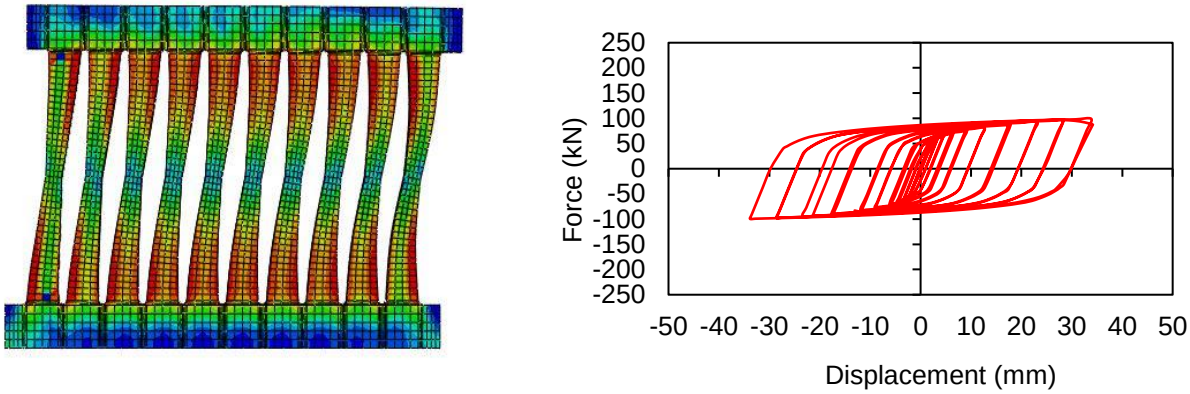

Figure 9: FE model and Hysteretic response for damper with b_c = 18mm, h = 270mm and t = 10mm

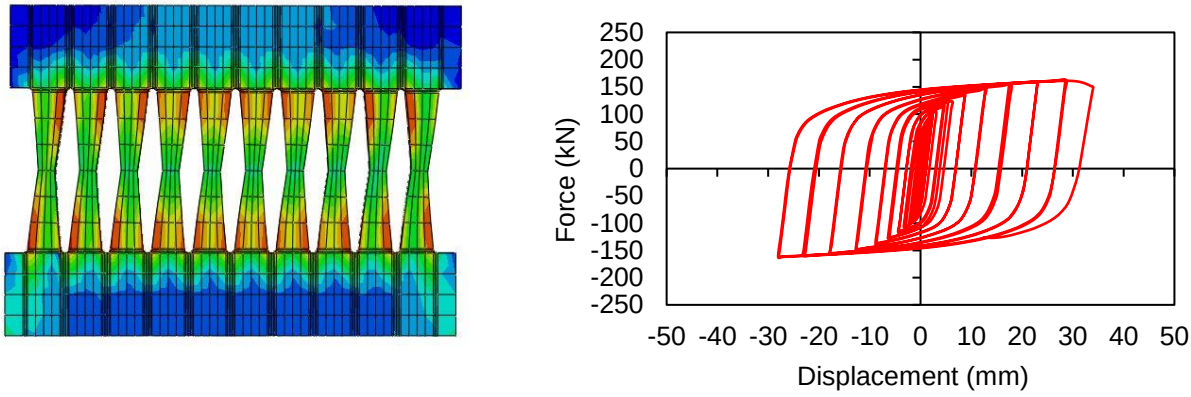

Figure 10: FE model and Hysteretic response for damper with b_c = 18mm, h = 180mm and t = 10mm

In Table 3, ductility (μ) is expressed as ratio of maximum displacement to yield displacement. From different parameter combination, the ductility for the specimens ranges from 5 to 68. The higher values of ductility are obtained from the specimen with thickness of 15 and 20mm. The total energy absorption

capacities (E) of the specimens were obtained adding the loop area of load-displacement hysteretic curve. On comparing energy absorption capacity from different geometrical shapes, the E value ranges from 1.2 to 7 times conventional slit damper.

Table 3: Summary of the structural characteristics

#	Factors			P_y (kN)	P_{max} (kN)	P_{min} (kN)	δ_y (mm)	δ_{max} (mm)	δ_{min} (mm)	μ	K_{eff} (kN/mm)	E (kN-mm)	β_{eff} (%)
	b_c	h	t										
1	9	90	10	94.38	158.60	-163.11	0.43	2.21	-2.38	5.09	70.15	4264	4.8
2	18	90	10	148.93	222.37	-230.81	0.59	3.32	-2.37	5.60	79.64	6304	3.9
3	36	90	10	172.89	337.98	-336.35	0.58	4.64	-4.65	8.06	72.62	19699	8.8
4	9	180	10	61.38	104.15	-105.77	1.21	11.98	-12.42	9.90	8.60	15868	30.3
5	18	180	10	104.13	162.23	-161.65	2.34	28.70	-27.88	12.26	5.72	109062	27.5
6	36	180	10	83.90	180.57	-179.09	1.00	28.72	-28.74	28.72	6.26	89344	23.4
7	9	270	10	38.46	69.68	-69.88	2.32	28.06	-28.69	12.09	2.46	38294	13.6
8	18	270	10	51.32	98.79	-33.86	2.18	33.86	-33.84	15.53	1.96	104819	11.6
9	36	270	10	54.85	103.93	-103.10	1.61	50.31	-50.30	31.25	2.06	172037	7.9
10	9	90	15	140.94	277.02	-277.53	0.43	6.44	-6.43	14.88	43.08	28843	14.9
11	18	90	15	221.20	431.95	-426.72	0.58	12.45	-9.02	21.47	39.99	83367	24.5
12	36	90	15	368.65	605.61	-592.76	1.11	12.40	-9.18	11.22	55.53	106513	19.3
13	9	180	15	101.86	161.65	-160.93	1.70	44.24	-44.92	26.02	3.62	215338	13.2
14	18	180	15	145.82	248.71	-247.57	1.91	50.10	-49.98	26.23	4.96	406378	16.6
15	36	180	15	105.79	261.55	-259.88	0.73	49.83	-49.96	68.26	5.23	457046	17.9
16	9	270	15	65.91	98.01	-97.43	3.31	49.68	-50.39	15.01	1.95	149553	6.8
17	18	270	15	78.76	151.24	-150.82	2.32	50.19	-50.04	21.63	3.01	224693	10.5
18	36	270	15	83.70	156.63	-157.92	1.66	50.06	-49.94	30.16	3.15	260131	11.5
19	9	90	20	188.38	367.26	-360.57	0.43	12.56	-12.83	29.00	28.67	102508	31.5
20	18	90	20	301.37	574.81	-568.04	0.62	17.92	-17.75	29.00	32.04	183487	23.8
21	36	90	20	438.73	818.14	-806.86	0.81	28.36	-28.76	35.14	28.45	604808	21.8
22	9	180	20	129.38	216.85	-215.49	1.29	44.72	-44.84	34.67	4.83	259403	17.1
23	18	180	20	164.56	329.56	-331.78	1.21	49.80	-50.08	41.16	6.62	541623	21.0
24	36	180	20	188.43	365.93	-363.90	1.66	49.66	-49.84	29.92	7.33	637535	24.2
25	9	270	20	77.06	133.46	-132.35	2.31	50.23	-50.01	21.74	2.65	201369	8.8
26	18	270	20	120.24	202.23	-201.69	3.17	49.63	-49.20	15.66	4.09	297749	12.1
27	36	270	20	119.86	216.32	-215.11	2.13	49.40	-50.02	23.19	4.34	347820	12.4

# denotes the no. of run

3 Response Surface Method (RSM)

In this study, with the aim of reducing the stress concentration at the end and increasing the damper performance, geometrical parameters such as strip width at mid height (b_c), height of the strip (h) and thickness (t) were chosen as critical variables. A response surface technique is applied to generate the regression equation for the effective stiffness and effective damping as a function of design variables (b_c, h and t). A second degree polynomial of the form shown in Equation 3 is used to setup relationship between effective stiffness, effective damping and shape variables x, (Montogomery 2008):

$$[3] \quad Y = \beta_0 + \sum_{i=1}^{n} \beta_i x_i + \sum_{i=1}^{n} \beta_{ii} x_i^2 + \sum_{i=1}^{n} \sum_{j=1}^{i} \beta_{ij} x_i x_j$$

where Y is response parameter, and β_0, β_i, β_{ij} are the regression coefficients. From the ANOVA, the effective stiffness (Equation 4) and effective damping (Equation 5) is expressed in terms of design parameter with regressions coefficients is given as:

$$[4] \quad K_{eff} = 5.13 + 1.05A - 24.17B - 6.73C - 0.79AB + 0.21AC + 10.91BC - 1.59A^2 + 20.92B^2 + 3.02C^2$$

$$[5] \quad \beta_{eff} = 20.82 + 0.29A - 3.26B + 2.30C + 0.20AB + 0.68AC - 5.03BC - 1.09A^2 - 7.49B^2 + 1.84C^2$$

where A, B and C are the strip width at mid height (b_c), height of the strip (h) and thickness of the damper (t) respectively and their second order interaction effects are given as (A^2, B^2, C^2, AB, AC and BC). From Equation 4 it is inferred that, height of the strip and thickness are the most influencing factor for the effective stiffness and from Equation 5, height of the strip has high contribution in predicting effective damping. Also, higher order and interaction effects between height of strip and thickness have an important role in estimating effective stiffness and damping. Figure 11 (a) to (f) presents the three dimensional response surface plot for responses (effective stiffness and damping) and shape parameters (b_c, h and t). From Figure 11 (a) and (c) it can be seen that, when the strip height (h) is between 180 and 90mm, effective stiffness increases gradually, in this region the specimen fails at very low displacement with high load irrespective of b_c and t of the specimen. At the same time, Figure 11 (e) indicates that by decreasing b_c around 18mm, stiffness of the specimen is reduced with thickness of 20mm and perform well at large deformations. Figure 11 (b) shows that, the specimen exhibits high damping when the height of strip is around 180mm with varying b_c and from Figure 11 (d), with specimen thickness 15 to 20mm and strip height around 180mm, the damping is greater than 20%. Also, from Figure 11 (f) it is clear that, by increasing t has high contribution in increasing the damping value for different b_c. Further, based on the ANOVA, the importance level of each factor is determined with F-test using Design Expert Software. The factors F-Value is calculated by dividing the model mean square with the residual mean square. The F-Value and their corresponding P-value with alpha level at 0.05 is shown in Table 4. If P-value less than 0.05, the factors has high influence on final response.

Table 4: Test Statistics Results

Effect	K_{eff} (KN/mm)		β_{eff} (%)	
	F-Value	P-Value	F-Value	P-Value
A	0.500	0.4884	0.044	0.8355
B	259.690	0.0001	5.340	0.0336
C	20.130	0.0003	2.660	0.1211
AB	0.200	0.6630	0.014	0.9082
AC	0.0140	0.9069	0.170	0.6888
BC	35.880	0.0001	8.640	0.0092
A^2	0.290	0.5972	0.160	0.6984
B^2	66	0.0001	9.590	0.0065
C^2	1.380	0.2564	0.580	0.4560

From Table 4, height of the strip and thickness are dominant factor in predicting the effective stiffness of the specimen, whereas, height of the strip is the most important factor for effective damping.

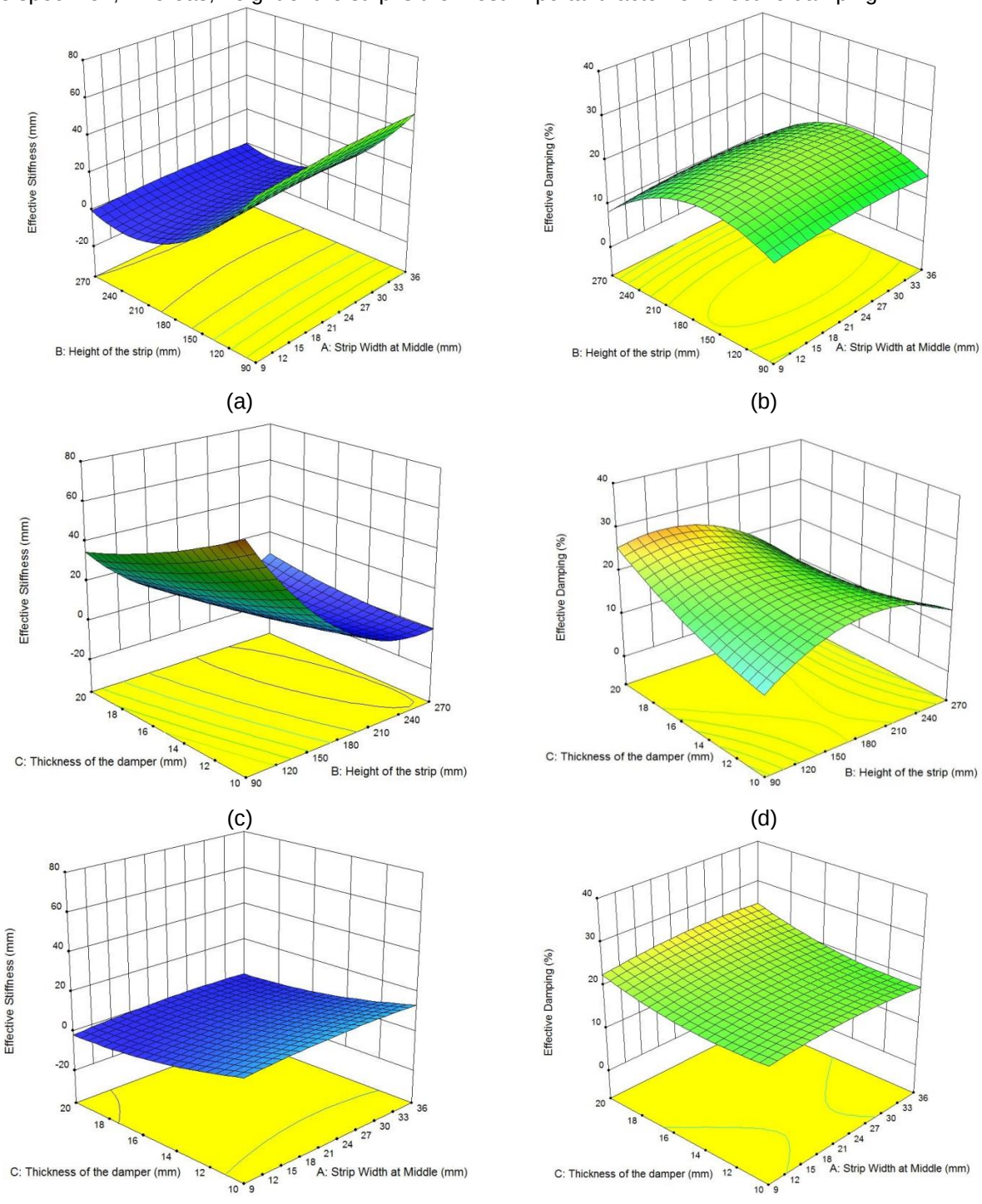

Figure 11 (a)-(f): Response surface plot between the responses (effective stiffness and effective damping) and shape parameters (b_c, h and t)

4 Conclusions

This study focussed about the effect of shape variables on the performance of conventional steel slit damper. Initially, a conventional steel slit damper is modeled numerically and validated with the experimental results. Further, a parametric study has been carried out for shape variables using design of experiment technique and response surface method was used to study about the interactions between the chosen parameters and final response. The following conclusions are made from this study:

1. Damper configuration with increased height of the strip has low stiffness and provides stable hysteretic curve under large displacement irrespective of strip width at mid height.
2. Reducing the strip width at the mid height has high influence on the damper performance by avoiding brittle damage at the end from stress concentration.
3. Effective damping of the modeled specimens was in the range of 10 to 25%. Further, varying the thickness and strip width at mid-height enhances the damping of the specimen when height of the strip is between 90 to 270mm.
4. Based on the response surface methodology, effective stiffness and effective damping is expressed as a function of strip width at mid-height (bc), height of the strip (h) and thickness of the damper (t).

References

Bergman, David M., and Goel, S.C., 1987. Evaluation of cyclic testing of steel-plate devices for added damping and stiffness. Department of Civil Engineering, University of Michigan, USA.

Chaboche, J.L., 1989. Constitutive equations for cyclic plasticity and cyclic viscoplasticity. *International Journal of plasticity*, 5(3), pp. 247-302.

Chan, R.W., and Albermani, F., 2008. Experimental study of steel slit damper for passive energy dissipation. *Engineering Structures*, 30(4), pp. 1058-1066.

Chang, K.C., Soong, T.T., Oh, S.T. and Lai, M.L., 1995. Seismic behavior of steel frame with added viscoelastic dampers. *Journal of structural engineering*, 121(10), pp. 1418-1426.

Constantinou, M.C., and Symans, M.D., 1993. Experimental study of seismic response of buildings with supplemental fluid dampers. *The Structural Design of Tall and Special Buildings*, 2(2), pp. 93-132.

Ghabraie K, Chan R., Huang, X., and Xie, YM., 2010. Shape optimization of metallic yielding devices for passive mitigation of seismic energy. *Engineering Structures*. 32(8), pp. 2258-2267.

Kobori, T., Miura, Y., Fukusawa, E., Yamada, T., Arita, T., Takenake, Y., Miyagawa, N., Tanaka, N., and Fukumoto, T., 1992. Development and application of hysteresis steel dampers. *In Proceedings of the 10th World Conference on Earthquake Engineering*, pp. 2341-2346.

Lee, C.H., Ju, Y.K., Min, J.K., Lho, S.H., and Kim, S.D., 2015. Non-uniform steel strip dampers subjected to cyclic loadings. *Engineering Structures*, 15(99), pp. 192-204.

Montgomery DC., 2008. Design and analysis of experiments. *John Wiley & Sons.*

Oh, S.H., Kim, Y.J., and Ryu, H.S., 2009. Seismic performance of steel structures with slit dampers. *Engineering structures*, 31(9), pp. 1997-2008.

Pall, A.S., Marsh, C., and Fazio, P., 1980. Friction joints for seismic control of large panel structures. *Journal of Prestressed Concrete*, 25(6), pp. 38–61.

Skinner, R.I., Kelly, J. and Heine, A., 1973. Energy absorption devices for earthquake resistant structures. *In Proceeding of the Fifth World Conference on Earthquake Engineering*, pp. 2924-2933.

Soong, T.T., Constantinou, M.C., 2014. Passive and active structural vibration control in civil engineering. *Springer.*

Teruna, D.R., Majid, T.A., and Budiono, B., 2015. Experimental study of hysteretic steel damper for energy dissipation capacity, *Advances in Civil Engineering*

Tsai, K.C., Chen, H.W., Hong, C.P., and Su, Y.F., 1993. Design of steel triangular plate energy absorbers for seismic-resistant construction. *Earthquake spectra*, 9(3), pp. 505-528.

Version, ABAQUS., 2011. 6.14-1. *Dassault Systemes Simulia Corp. RI, USA*

Whittaker, A.S., Bertero, V.V., Thompson, C.L., and Alonso, L.J., 1991. Seismic testing of steel plate energy dissipation devices. *Earthquake Spectra*, 7(4), pp. 563-604.

Yoshida, J., Abe, M., Fujino, Y., and Watanabe, H., 2004. Three-dimensional finite-element analysis of high damping rubber bearings. *Journal of engineering mechanics*, 130(5), pp. 607-620.